

# Reprocessability of self-healing polymer coatings based on Diels-Alder thermo-reversible chemistry

University of Groningen, BSc thesis, Michiel Frans Meindersma (S3464938)

We investigated reprocessability of self-healing thermosetting polymer coatings based on furan-grafted polyketones crosslinked with bis-maleimide. Mixtures of furan-grafted polyketones and bis-maleimide were prepared and spin coated onto glass plates. The coated glass plates were submerged into anthracene-solvent mixtures and the solutions underwent different thermal treatments (25, 50, 75, 100 and 120 °C) for 32h. During thermal treatment, UV-vis spectroscopy was used to follow furan-grafted polymer solubilization at different time intervals. It followed that all of the investigated solvents were able to solubilize (part of) the self-healing polymeric coating at different temperatures. At lower temperatures (25, 50 and 75 °C), the solubility/miscibility between the furan-grafted polymer and the apparent solvent appeared to be decisive in determining the order of solubilization for the examined solvents. At higher temperatures (100 and 120 °C), the reverse Diels-Alder reaction occurred to a larger extent. This diminished the thermosetting polymer network, thus increasing solubilization of furan-grafted polyketones for all solvents. It appeared that, at these higher temperatures, the relative solubility (estimated based on Hansen Solubility Parameters) of the solvents and furan-grafted polyketones was no longer decisive for the observed order of polymer solubilization. To our knowledge, the reprocessability of self-healing thermosetting polymer coatings has not been studied before. The observed reprocessability of such coatings might drive the replacement of conventional non-recyclable thermosets by self-healing polymeric systems.

This BSc thesis has been carried out during the COVID-19 global pandemic (spring-summer 2020). In order to comply with all the learning goals specified for the BSc final project in Chemical Engineering at the University of Groningen, (some of) the results presented in this thesis were not experimentally obtained but provided by the main supervisor based on previous unpublished data and personal experience, or obtained from published literature. The source of data has also been specified explicitly or referenced wherever they appear in this text.

## 1. Introduction

Of all processed polymers, 90 weight percent is accounted for by thermoplastics. The remaining polymers can be characterized as thermosets [1]. Thermosetting polymers undergo a crosslinking reaction ('curing') upon heating and are converted into an insoluble and infusible material. This insolubility and infusibility arise from the covalently crosslinked network structure that characterizes a thermoset. The spatial arrangement of the chemical crosslinks as well as the degree of crosslinking heavily affects the properties of the cured thermosetting polymer network that is formed [2].

The word 'reprocessing' will intentionally be used throughout this work rather than using 'recycling'. The reason for this lies in the in exact definition of both words. Recycling is defined as: "Separating, collecting, processing, marketing, and ultimately using a material that otherwise would have been disposed" [3]. Conversely, reprocessing is defined as: "To convert recovered materials into new raw materials that can be used to make finished goods" [3]. Given the above, it can be concluded that reprocessing focusses on the exact process required to accomplish re-use of recovered materials. On the contrary, recycling has a comprehensive definition including aspects ranging from separation to marketing. Consequently, the definition of reprocessing seems to correspond most to the polymer treatment described in this work.

Nowadays, thermosets are used for various applications including coatings, adhesives, electrical insulation and polymer composites [4]. The latter does not only apply for thermosets, because thermoplastics are used as composite materials as well [5]. However, the focus in this work will be on thermoset polymers. Generally, the aforementioned infusibility (or thermal-stability) and insolubility of thermoset materials are considered beneficial during the life-time of a thermoset. These properties distinguish thermosets from conventional thermoplastics, creating a separate market for thermoset applications [6]. Ironically, it is exactly these beneficial properties that complicate thermoset reprocessing upon completion of the application life-time [7]. Moreover, there is another factor that complicates thermoset reprocessing: the presence of additives such as fillers and fibrous reinforcements that results in polymer composites that are difficult or impossible to separate [4].

Nevertheless, literature mentions several methods that are currently available for thermoset reprocessing (Figure 1). *Fine grinding* is a method in which thermoset resins are simply grinded into powder which is used as a filler for new polymer matrices [8] [9]. Unfortunately, this method is not applicable for more advanced polymer composites as it causes an irretrievable loss in economic value [10]. Other than simple grinding, there are more advanced grinding methods that succeed in maintaining part of the thermoset properties. However, thermoset grinding generally results in thermoset fractions being used as low-value fillers in polymer composites [8] [9].

Another way to reprocess thermosets is by *chemical degradation* [9]. This method uses chemical agents to de-crosslink the aforementioned crosslinked network that characterizes thermosets. The method is applicable to a very limited part of the commercially available thermosets and it is known to be harmful towards reinforcements (fillers, fibers etc.) that are present in the polymer that is to be reprocessed [9]. Also, in most cases, only a part of the thermoset can be recovered whereas another part has to be discarded due to shattered mechanical properties [8].

Moreover, other methods include *pyrolysis* and *burning*. *Burning* cannot be considered as reprocessing as it just regains the heat of combustion of the thermoset polymer that is burnt [6]. *Burning* is a method that is not often applied as the heat of combustion is generally low for thermoset polymers [11]. *Pyrolysis* is a process in which the macromolecules (thermoset polymers) are heated to temperatures between 700 and 1000 °C under an inert atmosphere. This breaks down the crosslinked network structure and allows for regeneration of thermoset monomers for a small class of thermosets [6].

Nonetheless, landfill is still the most-used end-of-life option for thermoset products anno 2020 [12]. Reasons for the small-scale reprocessing of thermosets are the high-energy consumption that is often

required [6], the cost-intensive nature of the methods [10] and the lack of practical knowledge for currently available reprocessing techniques [13]. The work of Post and co-workers [12] mentions the need for reduced-energy reprocessing methods that allow for efficient thermoset reprocessing. Correspondingly, Zhang and co-workers reported the need for novel or more efficient methods for thermoset reprocessing [4].

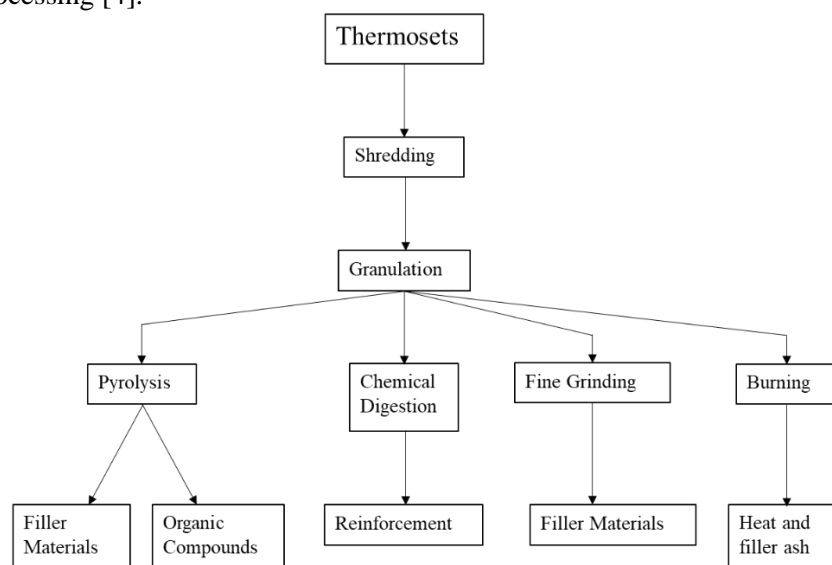


Figure 1| a schematic overview of different reprocessing methods applicable for thermoset polymers, based on the works of Balasubramanian [6] and Kulkarni [14].

Development of re-processable thermosets is a relatively new field or interest [12] [4]. According to the work of Post and co-workers [12], this could be a huge step forward in minimizing thermoset landfill. Amongst currently investigated self-healing systems, shown in Figure 2, are the reversibly crosslinked Diels-Alder polymers [4] [15] [16].

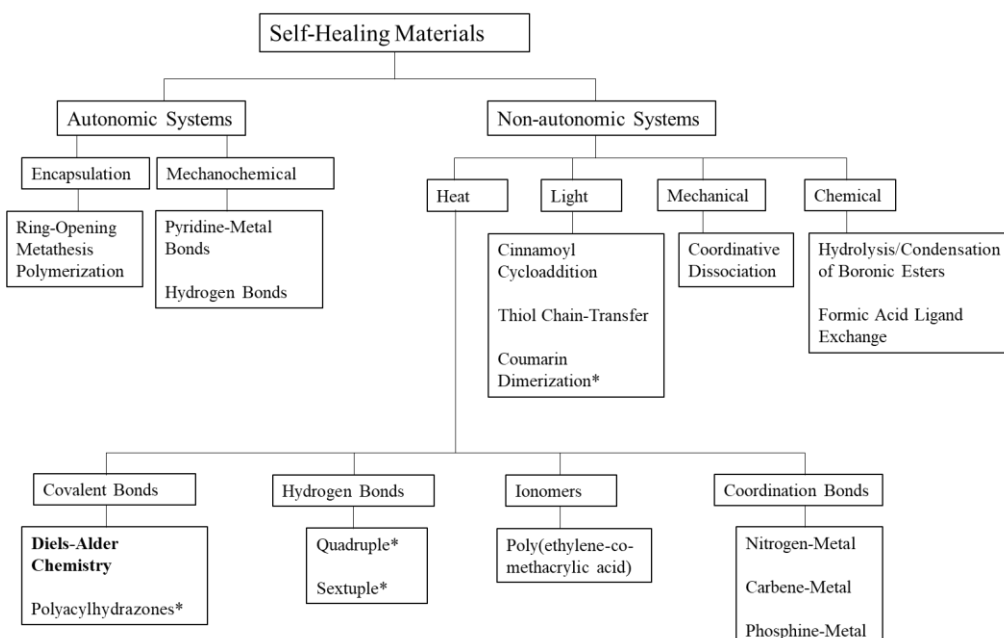


Figure 2| Organization of self-healing materials based on their chemistry. \* Indicates potential materials. This Figure was constructed based on the work of Williams and co-workers [17].

The Diels-Alder reaction is a [4+2] cycloaddition in which a conjugated diene adds to a substituted dienophile to yield cyclohexene derivatives [18]. The Diels-Alder reaction is considered to be a special case in the more general class of  $\pi$ -system reactions, the products of the Diels-Alder reaction are

generally called cycloadducts [19]. The fact that the reaction is characterized as a [4+2] cycloaddition originates from the amount of reacting  $\pi$ -electrons present in the diene and dienophile. The reacting diene contains two double bonds and therefore four  $\pi$ -electrons are involved in the reaction. Alternatively, the substituted dienophile contains one double bond and therefore only two  $\pi$ -electrons are involved in the reaction [18] [19]. The reaction mechanism of an example Diels-Alder reaction is shown in Figure 3.

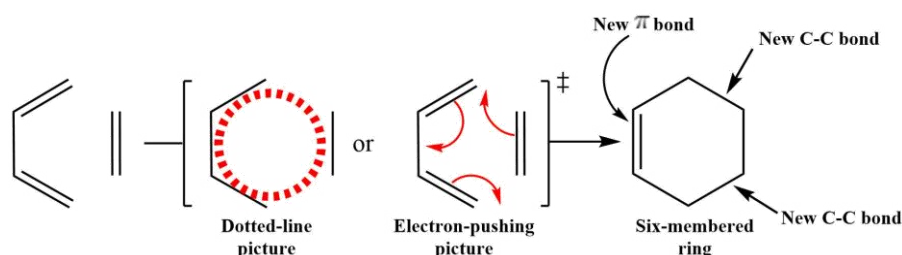


Figure 3| an example of the concerted Diels-Alder reaction mechanism scheme based on *Organic Chemistry: Structure and Function* [19].

However, for the particular example shown in Figure 3, the dienophile does not contain any significant substituents. Therefore, there will only be one product instead of a mixture of distinct stereoisomers. In general, the Diels-Alder reaction is known to be stereoselective [19]. Depending on the conformation (*cis* or *trans*) of the dienophile, different products will be formed. A rule of thumb states that the stereochemistry of the dienophile will be retained in the Diels-Alder product [18]. To clarify, if the dienophile has two substituents that are in the *cis*-conformation, these substituents will end up on the same side of the *endo*-cyclohexene product. In case the dienophile-substituents end up on different sides of cyclohexene ring, the so-called *exo*-product is formed [19]. An example of the stereoselective nature of the Diels-Alder reaction is given in Figure 4.

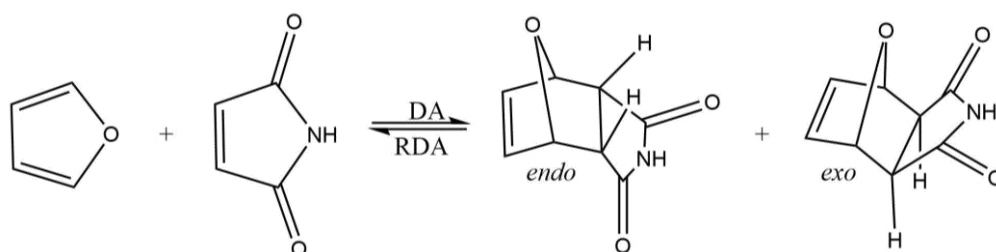


Figure 4| reaction equation showing the influence of the dienophile conformation on the conformation of the cyclohexene product, based on the work of Rulišek and co-workers [20].

Nowadays, the field of Diels-Alder chemistry receives a lot of attention within the scientific community. The reason for this lies in the variable substrate-scope, high yields and the thermo-reversibility of the Diels-Alder reaction [21]. The substrate-scope is determined by the chemical properties of the species involved in the Diels-Alder reaction. To illustrate, the conjugated dienophile generally needs to be electron-poor whereas the substituted diene needs to be electron-rich [19]. Consequently, it can be seen from Figure 4 that the diene contains an ether moiety which can be considered as electron-donating [19]. On the contrary, the dienophile contains two carbonyl groups that can be considered electron-withdrawing with respect to the dienophile double bond [22]. It follows, that furan-maleimide systems are very suitable to undergo the Diels-Alder reaction. Additionally, furan-maleimide Diels-Alder systems generally show thermo-reversibility at comfortable temperatures [4] [23]. As a result, furan and maleimide have received plenty of attention compared to other Diels-Alder pairs that have been investigated [24].

Other than the furan-maleimide pair shown in Figure 4, a lot of different substrate variations have been investigated for the Diels-Alder reaction [25]. As was mentioned above, the thermo-reversibility is one

of the factors that make Diels-Alder chemistry a worthwhile field of research. This thermo-reversibility as well as the temperatures at which it occurs are heavily affected by the substrates involved [26], the utilized solvents [27] and characteristics of the reacting polymers/molecules [4] [25]. Table 1 shows the forward and backward reaction temperature for several Diels-Alder pairs.

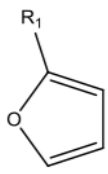
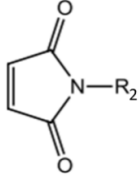
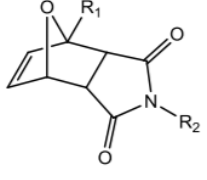
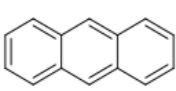
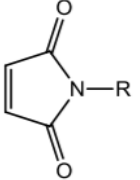
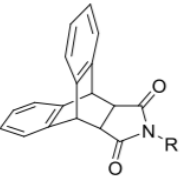


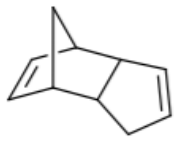
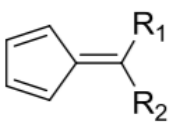
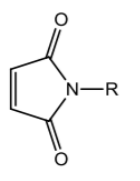
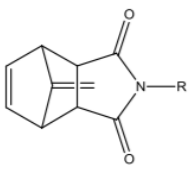
Diene	Dienophile	Adduct	T <sub>DA</sub> (°C)	T <sub>RDA</sub> (°C)	Ref.
 <i>Furan</i>			50-80	110-170	[4] [23] [28] [29]
 <i>Anthracene</i>			125	250*	[30] [31] [32] [33]
 <i>Cyclopentadiene</i>			25-120	150-215	[34] [35]
 <i>Fulvene</i>			30	50-100	[34] [36]

Table 1| different Diels-Alder reaction pairs and the temperatures of their forward and backward reaction. \* anthracene-maleimide adducts generally decompose rather than undergoing a reverse Diels-Alder reaction [31].

According to the work of Zhang and co-workers [4], integration of furan moieties into the polymeric backbone can be valuable. By integration of these moieties, the furan-grafted polymer that is obtained can be crosslinked via the thermo-reversible Diels-Alder reaction to yield a re-mendable polymer composite. Diels-Alder crosslinked polymeric materials have been investigated thoroughly [28] [33] [25] and are considered as suitable replacements for conventional thermoset polymers [4] [12] [24]. However, reprocessing of re-mendable Diels-Alder polymeric materials has not received much attention within the scientific community and reprocessing possibilities are still considered questionable [37].

Here, we investigated possible reprocessing of a Diels-Alder crosslinked polymeric material. Based on the procedure of Zhang and co-workers [4], furan-grafted polyketones (PK-FU) were synthesized and subsequently crosslinked using 1,1'-(methylene-di-1,4-phenylene)bis-maleimide (bis-maleimide). The resulting polymeric mixture was analysed using <sup>1</sup>H-NMR spectroscopy, FTIR spectroscopy and Elemental Analysis. The reactions involved are shown in Figure 5.

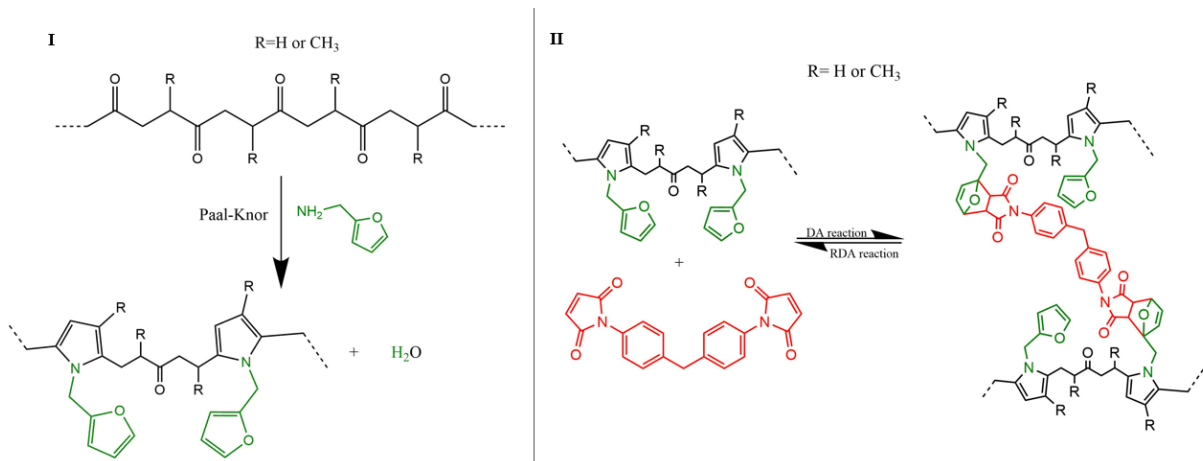


Figure 5| reaction equations for furan-grafting of polyketones via the Paal-Knorr reaction (I) and crosslinking of PK-FU via the Diels-Alder reaction (II), based on the work of Zhang and co-workers [4].

After synthesis and characterisation of crosslinked PK-FU, the polymeric material was spin coated onto different glass plates. The thermo-reversibility of the coated glass plates was demonstrated using DSC analysis. Additionally, the self-healing effect was indicated during thermal treatment of scratched coated glass plates. Subsequently, the reprocessability of the prepared polymer coating was examined. The work of Kim [38] indicated competitive behaviour of anthracene and furan moieties with respect to form a maleimide Diels-Alder adduct. This indicates the formation of an equilibrium situation in which furan moieties are constantly coupling- and decoupling anthracene and maleimide. However, Table 1 indicates the thermal stability of anthracene-maleimide adducts. Therefore, if the equilibrium would be investigated at relatively low temperatures (25-120 °C) the anthracene-maleimide adduct formation could be considered irreversible. Accordingly, addition of an anthracene-solvent mixture could drive the formed equilibrium into the ideal situation in which all maleimide is bound to anthracene. As a result, the PK-FU would be fully de-crosslinked and solubilization of this polymeric material could possibly be achieved. A schematic overview of the proposed reprocessing of a re-mendable PK-FU coating is given in Figure 6.

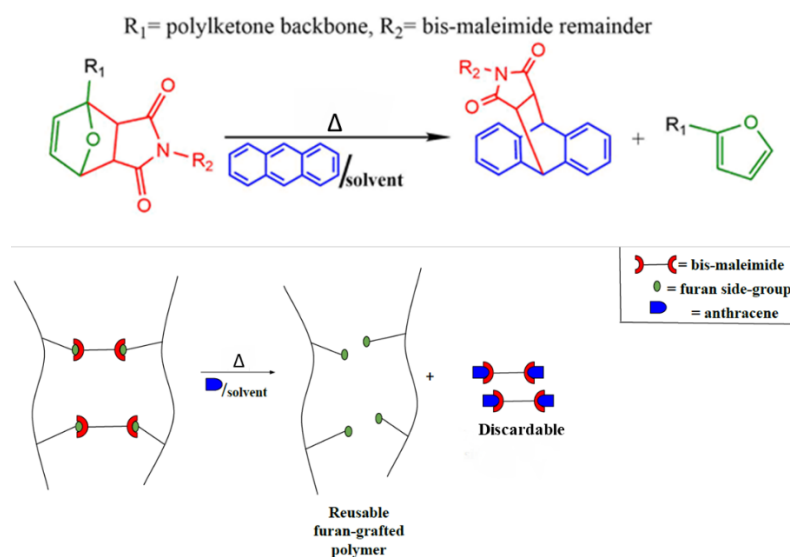


Figure 6| schematic overview of furan-grafted polymer reprocessing/solubilization using an anthracene-solvent solution.

## 2. Experimental Section

Given the above, we needed to find suitable solvents and conditions that could facilitate the proposed coating reprocessing. In order to predict which solvents would be suitable to dissolve both anthracene and the PK-FU, group-contribution methods from the work of Hansen were used [39]. The results of which are shown in Table 2. Based on this theoretical approach, four suitable solvents were identified: toluene, dimethyl formamide (DMF), tetrahydrofuran (THF) and chloroform. The solubilization of PK-FU was examined for all solvents, the detailed experimental steps are described below.

### 2.1 The synthesis of PK-FU.

The synthesis of the PK-FU was done following the procedure described in the work of Zhang and co-workers [4]. The experimental procedure is briefly described below.

A 250 mL round-bottom glass reactor was equipped with a reflux condenser, a U-type anchor impeller and an oil bath for heating. A  $^1\text{H-NMR}$  spectrum in  $\text{CDCl}_3$  was recorded for the polyketone (PK30) prior to the reaction. Subsequently, the polyketone (30 g) was liquified by preheating at the employed reaction temperature ( $100\text{ }^\circ\text{C}$ ) and furfurylamine (4.43 g, molar ratio 1:5 compared to PK30) was added in the first 10 min. Stirring was performed at 500 rpm and the reaction was carried out in bulk for 4h. After completion of the reaction, another  $^1\text{H-NMR}$  spectrum in  $\text{CDCl}_3$  was recorded for the resulting (reddish) mixture to determine the furfurylamine conversion. The remaining polymer mixture was washed several times using Milli-Q water in order to remove leftover furfurylamine. The resulting suspension was filtered and freeze-dried and reddish polymers were obtained as the final product. The resulting polymer was characterized by Elemental Analysis and FTIR spectroscopy. Elemental Analysis for PK-FU: Calcd: N, 1.95; Found: N, 1.72<sup>1</sup>.

### 2.2 Diels-Alder crosslinking of PK-FU and spin coating of glass plates.

A mixture of the PK-FU (2 g), the bis-maleimide (0.20 g) and chloroform (10 wt% polymer based on solvent) was prepared. 1,1'-(methylene-di-1,4-phenylene)bis-maleimide was used as crosslinker throughout experiments. The aforementioned mixture was spin coated (1200 rpm, 40 s) onto glass plates, the applied conditions were based on the work of Fortunato and co-workers [40]. Thermal treatment in an oven ( $50\text{ }^\circ\text{C}$ , 4-5 hrs) followed to ensure complete solvent evaporation and PK-FU crosslinking. Glass plates with a coating layer thickness of a couple of microns were obtained. A scalpel was used to get solid samples of the crosslinked PK-FU coatings on the glass plates. These solid state samples (approximately 10-15 mg) were used for differential scanning calorimetry (DSC) analyses at heating/cooling rates of  $10\text{ }^\circ\text{C}/\text{min}$  or  $20\text{ }^\circ\text{C}/\text{min}$ . Also a FTIR spectrum was recorded for the solid state samples. Additionally, several of the coated glass plates were scratched using a scalpel to examine the self-healing capacity of the damaged coating. Images were recorded for the scratched coating using an optical microscope. Subsequently, the glass plate underwent thermal treatment in an oven ( $120\text{ }^\circ\text{C}$ , 4-5 hrs) after which additional microscope images were collected. The flowchart in Figure 7 summarizes the preparation and examination of the coated glass plates.

---

<sup>1</sup> This result can be considered hypothetical/predicted. It was originally obtained by Elemental Analysis for a different polyketone formulation and has been modified for the performed research.



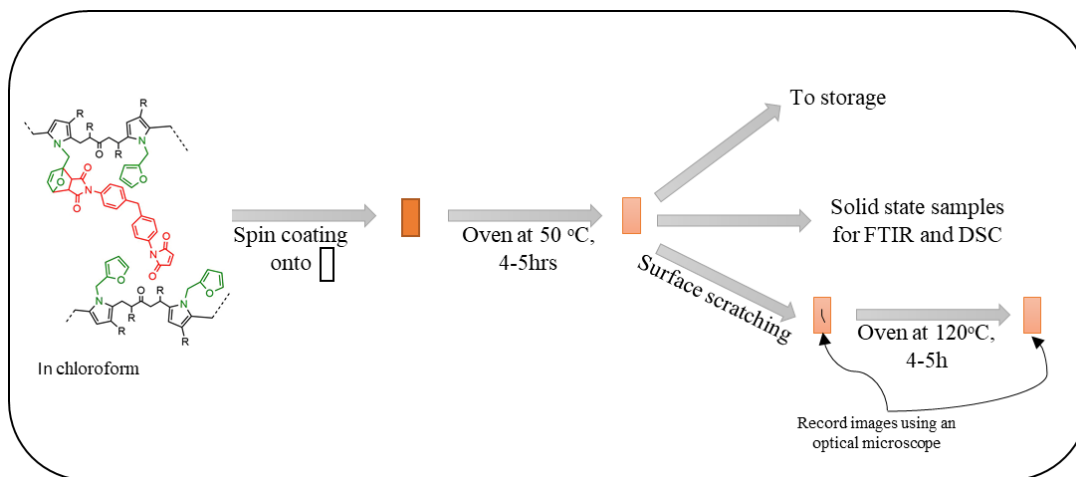


Figure 7| flowchart for the preparation and examination of polymer coated glass plates.

### 2.3 Determination of solubilization efficiency for PK-FU.

After preparation and examination of the coated glass plates, we started investigating possible reprocessability of the aforementioned coating. In order to do this, anthracene-solvent solutions needed to be prepared. Initially, we chose to saturate all solvents with anthracene rather than using solutions with a different anthracene concentration. Scanning Electron Microscopy (SEM) was used to get initial images of the cross section of the coated glass plates. Prior to exposure to the SEM electron beams, the coated glass plates were covered with several nano meters of gold. This was done in order to be able to harmlessly (for the sample and the equipment used) record SEM images. The coated glass plates were submerged in the prepared anthracene-solvent solutions in a closed vial and the system was allowed to settle for a sufficient amount of time. Subsequently, the submerged glass plates were exposed to different and distinct temperatures: RT, 50, 75, 100 or 120 °C. Heating, if necessary, was performed by using an oil bath. It was chosen to heat the different vials for 32h. During the heating, UV-vis spectra were recorded for the solvent-anthracene solution at different time intervals: 0h (after settling), 2h, 4h, 6h, 8h, 10h, 12h, 24h and 32h.

Based on the recorded UV-vis spectra, the furan-grafted polymer concentration in the different solvents was determined using the Lambert-Beer law.<sup>2</sup> Generally, the application of the Lambert-Beer law requires a proportional relationship between the absorbance and the concentration of a UV-vis sample. If the concentration of a sample becomes too high, this relationship may no longer be satisfied and the Lambert-Beer law may become inapplicable [41]. In case this happened, the UV-vis sample was diluted using the solvent that was already present in the UV-vis sample. After concentration determination based on the UV-vis spectrum of the diluted sample, dilution factors were used to obtain the concentration of the original sample. However, preliminary determination of the molar decadic extinction coefficient ( $\epsilon$ ) was needed in order to be able to relate the UV-vis absorbance and the polymer concentration. This was done by preparing mixtures of known PK-FU concentration for all different solvents. By recording UV-vis spectra for these mixtures, plots were obtained that showed the proportionality between the polymer concentration of a sample and its UV-vis absorbance. According to the Lambert-Beer law, the slope of the obtained graph equals the product of the molar decadic extinction coefficient and the pathlength of light travel in the cuvette ( $l$ ). As the pathlength of light travel in the cuvette was known, generally 1 cm, the molar decadic extinction coefficient could then be determined. Based on the different molar decadic extinction coefficients for all solvent-polymer combinations, the polymer concentration was calculated using the Lambert-Beer law.

<sup>2</sup> An example of the calculations involved is given in section A.4 of the Appendices.

Additionally, blank solutions of PK-FU and the different solvents (without anthracene) were prepared. These solutions underwent the same thermal treatment as the polymer-solvent-anthracene mixtures and were also characterized using UV-vis spectroscopy at different time intervals. This was done in order to determine the necessity of anthracene presence for PK-FU solubilization.

After 32 hours, the glass plates from the polymer-solvent-anthracene solutions were examined regarding coating dissolution using the naked eye. Also, SEM images were recorded for the glass plates and a <sup>1</sup>H-NMR spectrum in CDCl<sub>3</sub> was recorded for the anthracene-chloroform solution that had been heated to 120 °C. Figure 8 gives a schematic overview of the different experimental steps that were described.

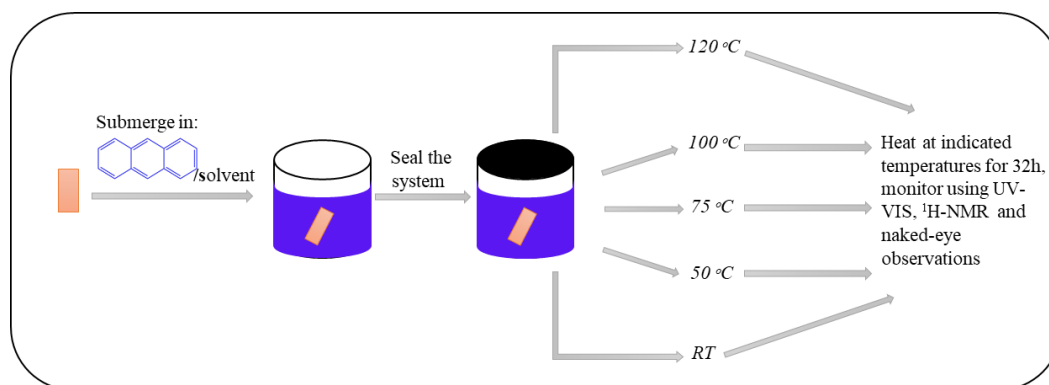


Figure 8| flowchart for the examination of anthracene-solvent and polymer-solvent miscibility at different temperatures.

Component	$\delta$ at 25 °C (MPa <sup>1/2</sup> )	Estimated $\delta$ at 25 °C (MPa <sup>1/2</sup> )	Boiling point (°C)
PK-FU	-	20.7 <sup>3</sup>	-
Anthracene	19.4 ([39])	19.6	340 ([42])
Toluene	18.3 ([39])	18.5	111 ([43])
Chloroform	18.9 ([39])	19.2	61 ([44])
Tetrahydrofuran	19.4 ([39])	19.6	65 ([45])
Dimethylformamide	24.0 ([39])	23.2	153 ([46])
Maleimide-anthracene adduct	-	15.9	-
Maleimide	-	14.7	-

Table 2| an overview of solvents with Hansen Solubility Parameters similar to both anthracene and the PK-FU. The boiling points of the solvents are also included for practical considerations. The solubility parameters in the middle column were estimated using group-contributions of first and second order groups according to a procedure described by Hansen [39].<sup>4</sup>

<sup>3</sup> Based on 15.4% furan-grating, the average of the carbonyl conversion calculated by <sup>1</sup>H-NMR spectroscopy (13.3%) and Elemental Analysis (17.5%).

<sup>4</sup> Detailed calculations are described in section A.3 of the Appendices.

### 3. Results and discussion

#### 3.1 Synthesis, characterisation and crosslinking of PK-FU.

In order to confirm the furan-grafting of the polyketones,  $^1\text{H-NMR}$  spectra were recorded for the polyketones before and after reaction with furfurylamine. The resulting  $^1\text{H-NMR}$  spectra are shown in Figure 9. From Figure 9, the inclusion of pyrrole and furan moieties into the polyketone backbone can be confirmed. Moreover, the characteristic signals for both the furan (5.9, 6.2 and 7.3 ppm) and the pyrrole groups (4.9 and 5.6 ppm) can be identified in the  $^1\text{H-NMR}$  spectrum of the PK-FU. Additionally, the carbonyl conversion was determined by comparing the integration of the polyketone backbone methyl group (1.1 ppm) with different product peaks<sup>5</sup>. This resulted in an average carbonyl conversion of 13.3%.

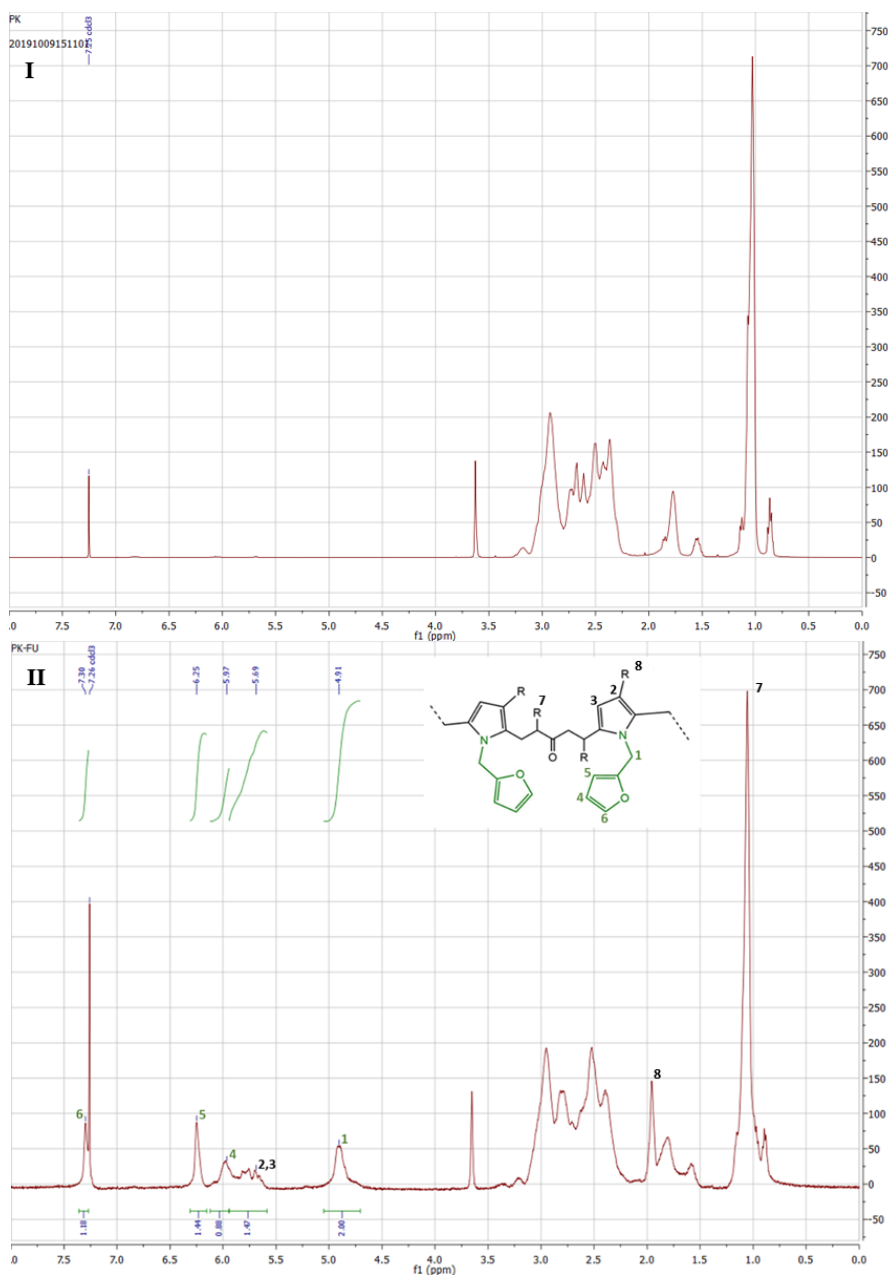


Figure 9|  $^1\text{H-NMR}$  spectra of polyketones before (I) and after (II) furan-grafting using furfurylamine. Based on furan-grafting of polyketones in the lab in an earlier stage.

<sup>5</sup> Detailed calculations are described in section A.1 of the Appendices.

The FTIR spectrum of the resulting polymer after furan-grafting is shown in Figure 10 (I). The spectrum is indicative for successful inclusion of pyrrole rings into the polymer backbone ( $1345$ ,  $1596$  and  $3112$   $\text{cm}^{-1}$ ). Moreover, the furan rings that originate from the furfurylamine with which the PK30 was reacted can be identified ( $1070$  and  $1345$   $\text{cm}^{-1}$ ). The Elemental Analysis (Calcd: N, 1.95; Found: N, 1.72<sup>2</sup>) was used to determine the furfurylamine conversion<sup>6</sup>: 87.5%. This corresponds to 17.5% furan grafting of the present carbonyl moieties. This conversion significantly disagrees with the conversion calculated by <sup>1</sup>H-NMR analysis (13.3%). The difference in obtained conversion can be caused by several factors. For example, slight measuring mistakes for the mass of the sample for Elemental Analysis heavily affect the obtained results. Correspondingly, the <sup>1</sup>H-NMR spectrum peak integration was performed manually and thus man-made mistakes might be present. And generally, the calculations that led to the aforementioned conversions are of simplified nature.

Crosslinking involves the Diels-Alder reaction of the furan groups of PK-FU and the bis-maleimide (Figure 5). Upon reaction, a C-O-C bond is formed. This bond can be used to distinguish the FTIR spectra of the crosslinked and the non-crosslinked polyketones. From Figure 10 (II), it can be seen that the intensity of the peak at  $1182$   $\text{cm}^{-1}$  significantly increases in comparison to (I). This implies the formation of the furan-maleimide adduct, and thus the crosslinking of PK-FU.

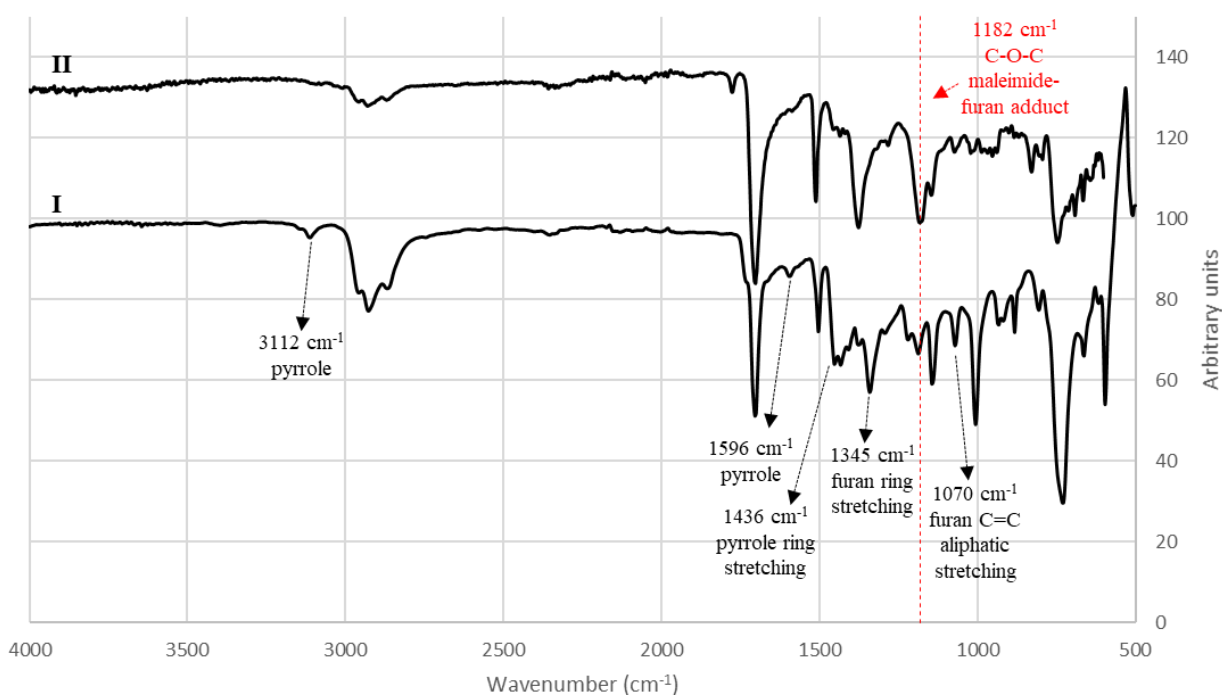


Figure 10| FTIR spectra for PK-FU before (I) and after (II) reaction with the bis-maleimide. Hypothetical/predicted spectra obtained from supervisor.

<sup>6</sup> Detailed calculations are described in section A.2 of the Appendices.

### 3.2 Examination of self-healing capacity and thermo-reversibility of the resulting polymer coating.

Optical microscope images, shown in Figure 11, indicate the capacity of the PK-FU coating to heal the surface to a substantial amount after one cycle of thermal treatment (120 °C, 4-5 hrs). This is indicative for the crosslinking-decrosslinking behaviour of the examined polymer coating.

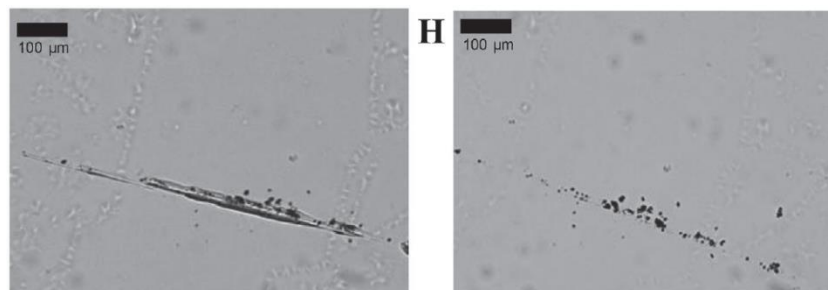


Figure 11| optical microscope images of the scratched (left) and the healed (right) coated glass plates, obtained from the work of Fortunato and co-workers [40].

The obtained DSC thermogram is shown in Figure 12. It can be seen that an exothermic transition is present for the investigated sample. This is indicative for the occurrence of the forward Diels-Alder reaction, which is described to be exothermic in literature [4]. The occurrence of the forward Diels-Alder reaction is indicative for the thermo-reversible crosslinking of the PK-FU.

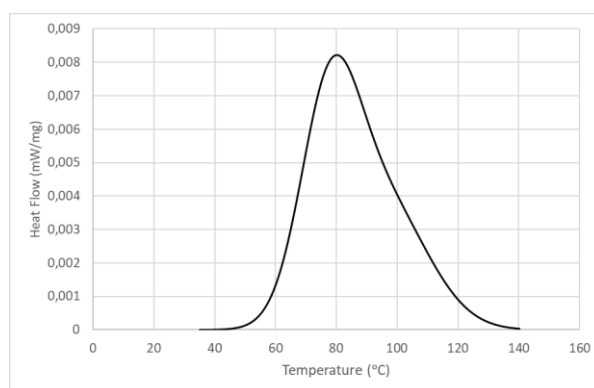


Figure 12| the thermal behaviour of the crosslinked PK-FU. Hypothetical/predicted thermogram obtained from the supervisor.

### 3.3 Examination of PK-FU solubilization.

The obtained UV-vis absorption was used to graph the concentration of PK-FU over time for different temperatures, the resulting plots are shown in Figure 13. It can be seen from Figure 13 that the concentration of PK-FU increases both with increasing time and temperature for all solvents. The observed time-dependency of solubilization is a well-known trend that is confirmed by literature [47]. The observed temperature-dependency can be explained based on knowledge on the different Diels-Alder reactions involved. Generally, elevation of the temperature facilitates the reverse Diels-Alder reaction for the crosslinked PK-FU [4]. Consequently, an increasing amount of non-crosslinked PK-FU (and bis-maleimide) will be present on the surface of the coated glass plates. This increased local concentration of non-crosslinked PK-FU is a driving factor for increased polymer solubilization. Additionally, anthracene can react with the liberated bis-maleimide molecules to form an adduct with high thermal stability [32]. Accordingly, the amount of bis-maleimide that is available for reaction with PK-FU decreases. This is another factor that increases the concentration of non-crosslinked PK-FU at the coating surface. Given the above, it can be concluded that (part of) this type of polymer coating can indeed be removed by submerging a coated surface in an anthracene-solvent solution and raising the temperature. Lastly, polymer solubilization is generally known to be facilitated by increasing the temperature of a polymeric mixture [48].

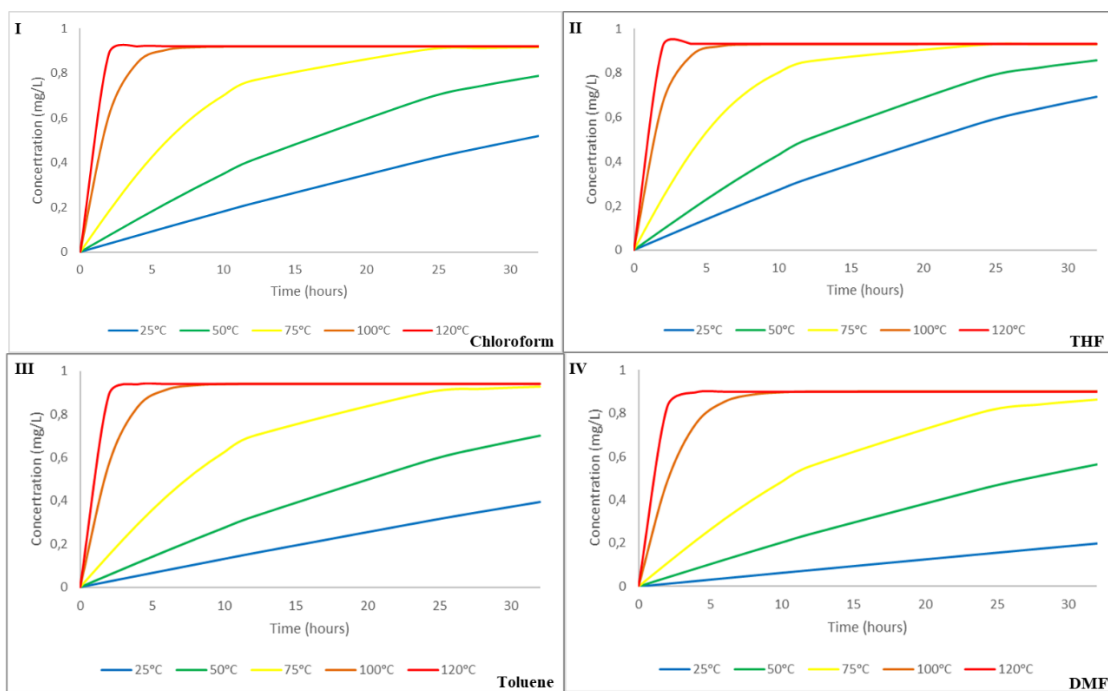


Figure 13| furan-grafted polymer concentration at different temperatures and time intervals for four different solvents: chloroform (I), THF (II), toluene (III) and DMF (IV). Hypothetical/predicted results obtained from the supervisor.

Within Figure 14, the aforementioned UV-vis results are categorised for all solvents at distinct temperatures. When looking at (I), (II) and (III) in Figure 14 it can be seen that the furan-grafted polymer concentration for all solvents shows a pattern. It can be observed that THF solubilizes PK-FU to the largest extent, thus resulting in the highest concentration in all three figures. Additionally, DMF shows the poorest furan-grafted polymer solubility, thus resulting in the lowest concentration in all three figures. The order of furan-grafted polymer concentration (and thus solubility) can be explained by comparing the estimated Hansen Solubility Parameters (hereafter HSP) shown in Table 2. Based on the absolute difference in HSPs (shown in (VI)) for the solvents and the furan-grafted polymer, a reliable order of polymer solubility for all solvents can be determined according to the work of David and co-workers [49]. A similar approach was taken in the work of Makoni and co-workers [50]. It can be seen that THF has the HSP that is closest to the HSP of the furan-grafted polymer, this explains the relatively

large concentration compared to the other solvents. On the contrary, the largest difference in solvent and furan-grafted polymer HSP is observed for DMF and thus the smallest concentration is observed in Figure 14. Lastly, the furan-grafted polymer concentration increases upon increasing temperature for all solvents. This observation follows the general trend for polymer solubilization mentioned in literature [48].

At higher temperatures ((IV) and (V)), the aforementioned order of solubility does not apply anymore. This is likely to be caused by interference of the formed maleimide-anthracene-solvent equilibrium. Solvents are known to be influential towards Diels-Alder reaction equilibria [27] and therefore a different order of concentration might have been formed. At relatively low temperatures, the reverse Diels-Alder reaction will not be present to a large extent. As a result, the crosslinked polymer network will be relatively intact and solvent penetration of this network will heavily depend on the miscibility of the solvent and the furan-grafted polymer. However, at high temperatures the reverse Diels-Alder reaction will induce significant de-crosslinking and therefore (part of) the polymeric network structure will be diminished. As the polymer network diminishes, solvent penetration will be facilitated for all solvents. This causes the observed pattern in (IV) and (V), in which the polymer concentration can no longer be predicted by the aforementioned HSPs. The work of Li and co-workers [51] confirms the influence of decreasing crosslinking density on the solubility parameters and the observed solubility of thermosets.

Additionally, SEM images were made for the cross section of the coated glass plates before and after submerging the plates into the different anthracene-solvent mixtures. Comparison of these SEM images yielded a clear conclusion: the coating was fully removed during treatment with any of the aforementioned anthracene-solvent mixtures.

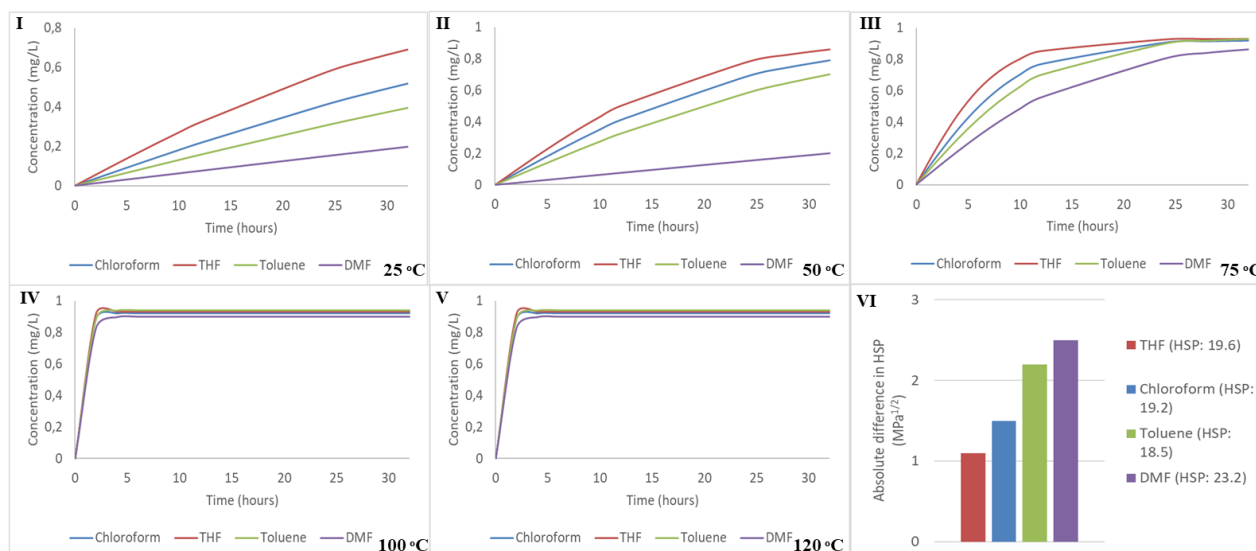


Figure 14| the absolute difference in the estimated Hansen Solubility Parameters for the solvents involved (VI) and the furan-grafted polymer concentration for all solvents at the indicated temperatures: 25 (I), 50 (II), 75 (III), 100 (IV) and 120 °C (V). Hypothetical/predicted results obtained from the supervisor.

Table 3 contains the peak shift and integration for important peaks in the <sup>1</sup>H-NMR spectrum obtained for a chloroform mixture after 32h of thermal treatment at 120 °C. From Table 3, the presence of PK-FU in chloroform can be confirmed. The furan groups corresponding to PK-FU are represented by the peaks at 6.0, 6.25 and 7.30 ppm. Similar relative integration values and peak shifts can be observed for these groups in the <sup>1</sup>H-NMR spectrum of PK-FU that was recorded in an earlier stage (Figure 9 (II)). Additionally, the presence of pyrrole moieties for the PK-FU can be observed (4.9, 1.96 and 5.5-5.8 ppm). Other than PK-FU, peaks can be assigned to anthracene (7.5, 8.0 and 8.44 ppm). And finally, the Diels-Alder adduct of anthracene and bis-maleimide can be identified (Table 3, **C1-C7**). The obtained



integration for all different components can be used to determine the relative composition of the final chloroform mixture.

Based on the  $^1\text{H-NMR}$  spectrum in Table 3, a molar ratio of 1:4.1:10.4 was determined for respectively the maleimide-anthracene adduct, furan groups in PK-FU and anthracene. This can be explained by the described experimental procedure. All examined solvents were saturated with anthracene, thus resulting in the observed excess. The ratio of the maleimide-anthracene adduct and the furan-groups indicate that slightly less than one adduct is formed per four furan-groups in PK30. This can be explained by the ratio that was used for addition of the bis-maleimide to the PK-FU. As 1 mol of bis-maleimide was added for every 4 mols of furan groups, the maximum ratio between furan and the aforementioned adduct amounts to 1:4. Judging from the obtained ratio, the reaction between anthracene and bis-maleimide approached completion after 32h.

## I

Peak shift (ppm)	Integration	Number of corresponding chemical group	Peak shift (ppm)	Integration	Number of corresponding chemical group
0.9-1.2	100	A7	6.00	8.92	A4
1.60	X	-	6.25	10.34	A5
1.80	X	-	7.06	17.40	C1
1.96	16.51	A8	7.25	17.40	C2
2.2-3.2	X	-	7.26	$\text{CDCl}_3$	-
3.70	X	-	7.30	X	A6
3.72	4.35	C7	7.37	8.70	C6
4.71	8.70	C4	7.50	90.00	B1
4.90	15.33	A1	7.67	8.70	C5
5.18	8.70	C3	8.00	90.00	B2
5.5-5.8	X	A2,A3	8.44	45.00	B3

## II

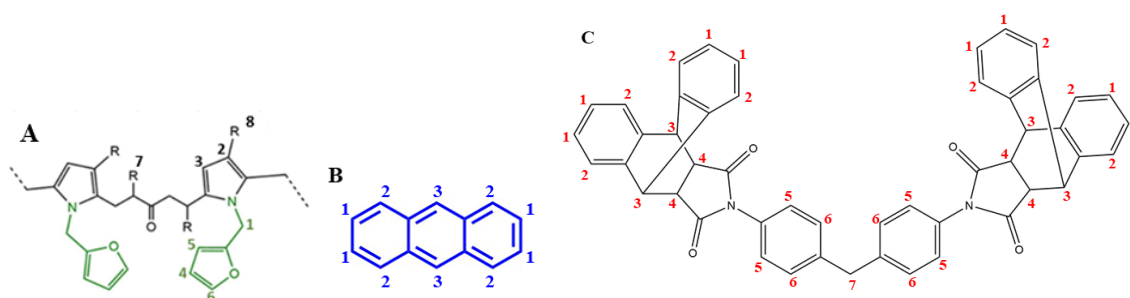


Table 3| (I) schematic overview of the peak shifts and the corresponding peak integration for the  $^1\text{H-NMR}$  spectrum obtained after examination of PK-FU solubilization in chloroform at 120 °C for 32h. X indicates signals that show a messy integration or signals that are not of importance. The given peaks are hypothetical/predicted results obtained from the supervisor. (II) figures illustrating which peak belongs to which part of the different chemical structures involved.

Apart from the fact that coating removal appeared to be possible using the aforementioned methods, practical considerations need to be discussed. It can be seen from the graphs in Figure 14 that the maximum concentration of polymer in the different solvents stays below 1 mg/L. This can be explained by the fact that the full coating has been dissolved at these points in time. If scale-up of the described procedure is desired, tremendous amounts of solvent might be needed in case the apparent polymer concentration does not greatly exceed the relatively low concentration [52] shown in Figure 14. Utilization of large amounts of solvents might not only be cost-intensive but also dangerous depending on the kind of solvent used. To illustrate, chloroform and THF are suspected carcinogens [44] [45] and



large-scale use of these solvents might be harmful towards people involved in the coating removal process. Moreover, large-scale execution of the described procedure might induce significant pressure built-up for solvents at operation temperatures above their boiling points (Table 2). Practically, it will not be possible to fully seal the system due to the assumedly large pressure built-up. Therefore, it might only be possible to execute the described procedure below the boiling point of the solvents involved. This would imply that the higher temperatures could only be applied for DMF (100, and 120 °C) and toluene (100 °C). Additionally, the process typically yields a mixture of the solvent, the furan-grafted polymer, the maleimide-anthracene adduct and anthracene (Table 3). Successful separation of these components is needed in order to be able to re-use furan-grafted PK30 (or other formulations) for coating applications. Critical assessment of separation methods will be needed in order to arrive at a method that can successfully perform the aforementioned separation.

### 3.4 Perspectives for further research

As was stated at the beginning of this work, the COVID-19 global pandemic has made execution of the described experiments impossible. The results presented are either hypothetical or literature-based and unfortunately none of the described research has actually been performed. Therefore, this thesis can be considered as a detailed pre-experimental form of research. Whenever it is possible to execute lab work again, it could therefore be interesting to execute the described experiments. As was stated in this thesis, increased reprocessability of self-healing polymeric systems might be a driving factor in replacing non-recyclable thermoset polymers. Other than executing the described experiments, it might be interesting to study the isolation of PK-FU from the mixtures obtained after thermal treatment. According to the described <sup>1</sup>H-NMR spectrum (Table 3) of the anthracene-chloroform mixture, the final mixture contains anthracene and the anthracene-maleimide adduct apart from the solvent and the desired PK-FU. If the described experiments were executed, we believe that this could indeed be the composition of the obtained mixtures. In order to be able to successfully re-use PK-FU for coating applications, anthracene and the described Diels-Alder adduct as well as the solvent need to be removed. Below, a proposed procedure for polymer isolation is described. It might be interesting to address the success rate of this isolation method.

From Table 2, it can be seen that both the maleimide-anthracene adduct and anthracene have lower HSPs than PK-FU. Therefore, upon addition of a small amount of a relatively polar compound like ethanol (HSP: 26.1 [39]), anthracene and the anthracene-maleimide adduct are likely to precipitate. After precipitation of these components, the resulting mixture can be filtered to obtain a filtrate in which (in the most ideal situation) only PK-FU and the solvent are present. Subsequently, the polymer-solvent mixture can undergo rotary evaporation in order to remove the residual solvent. Finally, a <sup>1</sup>H-NMR spectrum in CDCl<sub>3</sub> can be recorded for the reddish final product in order to determine its purity. Other than this, Size Exclusion Chromatography (SEC) might be a useful tool for isolating PK-FU from present impurities [53].

Other than studying polymer isolation, it might be interesting to alter several variables involved in polymer solubilization. To illustrate, for this work it was chosen to use anthracene-saturated solvent mixtures for coating removal. It might be interesting to investigate coating removal using solvents of known (non-saturated) anthracene concentration. Moreover, different amounts of solvent can be used for coating removal and it might be interesting to look into the use of (more) eco-friendly solvents. Also, for the described research it was chosen to solely use furan-grafted PK30. It might be of value to investigate coating solubilization of coatings based on different polyketones (e.g. furan-grafted PK0 or -PK50) or even different furan-grafted polymers (e.g. polyacrylates). Additionally, the influence of the crosslinking density of the involved polymer on coating solubilization could be studied by altering the molar ratio of bis-maleimide and furan-grafted polymer used. And finally, it could be interesting to investigate spray application of the anthracene-solvent solutions onto the coating and examine coating removal for this specific case.

#### 4. Conclusion

We developed a procedure for processing of self-healing thermosetting coatings based on furan-grafted polyketones and bis-maleimide. Using anthracene-solvent solutions, solubilization of the aforementioned polymeric coating was investigated for different thermal treatments (25, 50, 75, 100 and 120 °C) during 32h. Successful (partial) solubilization of the prepared polymer coatings was observed for all anthracene-solvent mixtures at all different thermal treatments. Additionally, the influence of the different temperatures that were applied could be addressed. It followed that, at lower temperatures (25, 50 and 75 °C), the solubility/miscibility of the apparent solvent and the furan-grafted polyketones was decisive for the observed order of solubilization for the different solvents. At higher temperatures (100 and 120 °C), the reverse Diels-Alder reaction occurred to a larger extent and the thermosetting polymeric network structure was (partly) diminished. Due to the decreased crosslinking density, solubilization of furan-grafted polyketones was facilitated for all solvents. Additionally, it was observed that the order of solubilization of furan-grafted polyketones was no longer determined by the solubility/miscibility of the apparent solvent and the aforementioned polymer. We hope that increased knowledge on reprocessability of self-healing polymeric systems, as described in this work, drives replacement of non-recyclable thermosets by the aforementioned polymeric systems.

## **Acknowledgements**

My sincere thanks goes to Felipe Orozco Gutierrez, without him it would not have been possible to finalize this work. His theoretical advice, insightful discussions and answers to my many questions have been essential for allowing me to further advance in the described research. Additionally, I would like to address my gratefulness towards Dr. Ranjita Bose. Not only has she helped to plan the different stages of my project, but she also supplied me with useful literature and guidelines regarding the structural framework of my thesis. Finally, I would like to thank prof. dr. A.A.Broekhuis who has helped me to get a first glimpse on self-healing Diels-Alder chemistry in the premature phase of my project.

## References

- [1] G. Challa, *Polymer Chemistry: An Introduction*, 1993.
- [2] D. Ratna, *Handbook of Thermoset Resins*, Shrewsbury: iSmithers, 2010.
- [3] The Association of Plastics Recyclers, "Plastics Recycling Glossary," 2008. [Online]. Available: [https://plasticsrecycling.org/images/pdf/design-guide/Plastics\\_Recycling\\_Glossary.pdf](https://plasticsrecycling.org/images/pdf/design-guide/Plastics_Recycling_Glossary.pdf). [Accessed 3 June 2020].
- [4] Y. Zhang and F. B. A. Picchioni, "Thermally Self-Healing Polymeric Materials: The Next Step to Recycling Thermoset Polymers?," *Macromolecules*, no. 42, pp. 1906-1912, 2009.
- [5] E. Gamstedt and L. Berglund, *Fatigue in Composites*, vol. *Fatigue of Thermoplastic Composites*, Woodhead Publishing, 2003.
- [6] Balasubramanian, *Composite Materials and Processing*, Boca Raton: CRC Press, 2013.
- [7] K. Yu, P. Taynton and W. Zhang, "Reprocessing and recycling of thermosetting polymers based on bond exchange reactions," *Royal Society of Chemistry*, no. 4, pp. 10108-10117, 2014.
- [8] J. Scheirs, *Polymer Recycling Science Technology and Applications*, Wiley, 1998.
- [9] F. La Mantia, *Handbook of Plastics Recycling*, iSmithers, 2002.
- [10] J. Simmons, "Recycling Thermoset Composites," *Reinforced Plastics*, vol. 10, no. 43, pp. 64-64, 1991.
- [11] R. Walters and S. Hackett, "Heats of Combustion of High Temperature Polymers," *Fire and Materials*, vol. 5, no. 24, pp. 245-252, 2000.
- [12] W. Post, A. Susa and R. Blaauw, "A Review on the Potential and Limitations of Recyclable Thermosets for Structural Applications," *Polymer Reviews*, vol. 2, no. 60, pp. 359-388, 2020.
- [13] Y. Liu, M. Farnsworth and A. Tiwari, "A review of optimisation techniques used in the composite recycling area: State-of-the-art and steps towards a research agenda," *Cleaner Production*, no. 140, pp. 1775-1781, 2017.
- [14] G. Kulkarni, "Introduction to Polymer and Their Recycling Techniques," *Recycling of Polyurethane Foams*, pp. 1-16, 2018.
- [15] J. Li, G. Zhang, R. Sun and C.-P. A. Wong, "Covalently Cross-Linked Reduced Functionalized Graphene Oxide/Polyurethane Composite Based on Diels-Alder Chemistry and Its Potential Application in Healable Flexible Electronics," *Materials Chemistry*, no. 5, pp. 220-228, 2017.
- [16] U. Lafont, C. Moreno-Belle, H. van Zeijl and S. van der Zwaag, "Self-Healing Thermally Conductive Adhesives," *Intelligent Material Systems and Structure*, no. 25, pp. 67-74, 2014.
- [17] K. Williams, D. Dreyer and C. Bielawski, "The Underlying Chemistry of Self-Healing Materials," *MRS Bulletin*, no. 33, pp. 759-765, 2008.

- [18] M. Gregoritz and F. Brandl, "The Diels–Alder reaction: A powerful tool for the design of drug delivery systems and biomaterials," *European Journal of Pharmaceutics and Biopharmaceutics*, no. 97, pp. 438-453, 2015.
- [19] P. Vollhardt and N. Schore, *Organic Chemistry: Structure and Function*, New York: W.H. Freeman, 2018.
- [20] L. Rulíšek, P. Sebek and Z. Svatos, "An Experimental and Theoretical Study of Stereoselectivity of Furan-Maleic Anhydride and Furan-Maleimide Diels-Alder Reactions," *Organic Chemistry*, vol. 16, no. 70, pp. 6295-6302, 2005.
- [21] H. Sun, C. Kabb and Y. Dai, "Macromolecular metamorphosis via stimulus induced transformations of polymer architecture," *Nature Chemistry*, 2017.
- [22] I. Varma and V. Gupta, "Thermosetting Resin Properties," *Comprehensive Composite Materials*, vol. 1, no. 56, p. 40, 2000.
- [23] A. Gandini, D. Coelho and A. Silvestre, "Reversible click chemistry at the service of macromolecular materials. Part 1: Kinetics of the Diels–Alder reaction applied to furan–maleimide model compounds and linear polymerizations," *European Polymer Journal*, vol. 12, no. 44, pp. 4029-4036, 2008.
- [24] L. Polgar and M. van Duin, "Use of Diels–Alder Chemistry for Thermoreversible Cross-Linking of Rubbers: The Next Step toward Recycling of Rubber Products?," *Macromolecules*, vol. 19, no. 48, pp. 7096-7105, 2015.
- [25] A. Gandini, "The furan/maleimide Diels–Alder reaction: A versatile click–unclick tool in macromolecular synthesis," *Polymer Science*, no. 38, pp. 1-29, 2013.
- [26] A. van Halteren, "Thermally Self-Healing Polymeric Materials," RUG, Groningen, 2018.
- [27] A. Widstrom and B. Lear, "Structural and solvent control over activation parameters for a pair of retro Diels-Alder reactions," *Nature Research*, no. 9, 2019.
- [28] X. Chen, M. Dam, K. Ono and A. Mal, "A Thermally Re-mendable Cross-Linked Polymeric Material," *Science*, no. 295, pp. 1698-1702, 2002.
- [29] J. Canadell, H. Fischer and G. De With, "Stereoisomeric effects in thermo-remendable polymer networks based on Diels-Alder crosslink reactions," *Polymer Chemistry*, vol. 15, no. 48, pp. 3456-3467, 2010.
- [30] M. Grigoras and G. Colotin, "Copolymerization of a bisanthracene compound with bismaleimides by Diels–Alder cycloaddition," *Polymer International*, no. 50, pp. 1375-1378, 2001.
- [31] J. Jones, C. Liotta and D. Collard, "Cross-Linking and Modification of Poly(ethylene terephthalate-co-2,6-anthracenedicarboxylate) by Diels–Alder Reactions with Maleimides," *Macromolecules*, vol. 18, no. 32, pp. 5786-5792, 1999.

- [32] M. Grigoras, M. Sava, G. Colotin and C. Simionescu, "Synthesis and Thermal Behavior of Some Anthracene-Based Copolymers Obtained by Diels–Alder Cycloaddition Reactions," *Wiley InterScience*, 2007.
- [33] H. Durmaz, B. Colakoglu, U. Tunca and G. Hizal, "Preparation of Block Copolymers Via Diels Alder Reaction of Maleimide- and Anthracene-End Functionalized Polymers," *Journal of Polymer Science*, no. 44, pp. 1667-1675, 2006.
- [34] A. Peterson and G. Palmese, *Click Chemistry for Biotechnology and Materials Science*, vol. Chapter 9, Wiley, 2009, pp. 169-214.
- [35] E. Murphy, E. Bolanos and F. Wudl, "Synthesis and characterization of a single-component thermally remendable polymer network: Staudinger and Stille revisited," *Macromolecules*, vol. 14, no. 41, pp. 5203-5209, 2008.
- [36] P. Boul, P. Reutenauer and J. Lehn, "Reversible Diels-Alder reactions for the generation of dynamic combinatorial libraries," *Organic Letters*, vol. 1, no. 7, pp. 15-18, 2005.
- [37] S. Ma and D. Webster, "Degradable thermosets based on labile bonds or linkages: A review," *Progress in Polymer Science*, no. 76, pp. 65-110, 2018.
- [38] H. J. Kim, "Systematic Study on Reaction Dynamics of Furan, Maleimide and Anthracene for responsive polymer applications," University of Groningen, Groningen, 2020.
- [39] C. Hansen, *Hansen Solubility Parameters: A User's Handbook*, CRC Press, 2007.
- [40] G. Fortunato, E. Tatsi, B. Rigatelli and S. Turri, "Highly Transparent and Colorless Self-Healing Polyacrylate Coatings Based on Diels-Alder Chemistry," *Macromolecular Materials and Engineering*, 2020.
- [41] B. Herzog, A. Schultheiss and J. Giesinger, "On the Validity of Beer-Lambert Law and its Significance for Sunscreens," *Photochemistry and Photobiology*, vol. 2, no. 94, pp. 384-389, 2018.
- [42] PubChem, "Anthracene," PubChem, 2020. [Online]. Available: <https://pubchem.ncbi.nlm.nih.gov/compound/8418>. [Accessed 6 May 2020].
- [43] PubChem, "Toluene," PubChem, 2020. [Online]. Available: <https://pubchem.ncbi.nlm.nih.gov/compound/7843>. [Accessed 19 March 2020].
- [44] PubChem, "Chloroform," PubChem, 2020. [Online]. Available: <https://pubchem.ncbi.nlm.nih.gov/compound/6212#section=Taste>. [Accessed 6 May` 2020].
- [45] PubChem, "Tetrahydrofuran," PubChem, 2020. [Online]. Available: <https://pubchem.ncbi.nlm.nih.gov/compound/8028#section=Boiling-Point>. [Accessed 6 May 2020].
- [46] PubChem, "Dimethylformamide," PubChem, 2020. [Online]. Available: <https://pubchem.ncbi.nlm.nih.gov/compound/6228#section=Boiling-Point>. [Accessed 6 May 2020].

- [47] S. Gaikwad, R. Mhalaskar and Y. Mahale, "Review on: Solubility Enhancement of Poorly Water Soluble Drug," *Indo American Journal of Pharmaceutical Research*, pp. 5530-5541, 2014.
- [48] G.Challa, *Polymer Chemistry An Introduction*, 2019.
- [49] D. David and T. Sincock, "Estimation of miscibility of polymer blends using the solubility parameter concept," *Elsevier*, vol. 21, no. 33, pp. 4505-4514, 1992.
- [50] P. Makoni, K. WaKasongo and Khamanga, "The use of quantitative analysis and Hansen solubility parameter predictions for the selection of excipients for lipid nanocarriers to be loaded with water soluble and insoluble compounds," *Saudi Pharmaceutical*, 2020.
- [51] C. Li and A. Strachan, "Cohesive energy density and solubility parameter evolution during the curing of thermoset," *Polymer*, vol. 135, no. 180, pp. 162-170, 2017.
- [52] D. Wang, "Polymer Flooding Practice in Daqing," *Enhanced Oil Recovery Field Case Studies*, pp. 83-116, 2013.
- [53] B. Trathnigg, "Size Exclusion Chromatography of Polymers," in *Encyclopedia of Analytical Chemistry*, Graz, 2006.
- [54] D. van Krevelen and K. te Nijenhuis, *Properties of Polymers, Fourth Edition: Their Correlation with Chemical Structure; their Numerical Estimation and Prediction from Additive Group Contributions*, vol. Chapter 7: Cohesive Properties and Solubility, Amsterdam: Elsevier, 2009.

## Appendices

### A.1 Furfurylamine conversion using the <sup>1</sup>H-NMR spectrum

Peak chemical shift (ppm)	Integration	# of protons corresponding to the signal	Normalized integration	Furfurylamine conversion
1.1	1	3	0.48	-
1.9	0.16	3	0.076	0.138
4.9	0.13	2	0.065	0.120
5.9	0.070	1	0.070	0.128
6.2	0.080	1	0.080	0.144

Table A-1| overview of different peaks from the <sup>1</sup>H-NMR spectrum for PK-FU.

Using the obtained <sup>1</sup>H-NMR spectrum for PK-FU (Figure 9 (II)), the furfurylamine conversion can be approximated. The peaks at the ppm-values given in Table A-1 were integrated using Mestrenova 10.0.2 (hereafter Mestrenova). By comparison of the polymer backbone methyl peak (1.1 ppm) and the given product peaks, the conversion can be approximated. The calculation of the furfurylamine conversion consisted of several steps, the formulas applied in the different steps are given below.

*Step 1: normalization of the integrations obtained from Mestrenova*

$$\text{normalized integration} = \frac{\text{integration from Mestrenova}}{\# \text{ protons corresponding to the integrated peak}}$$

*Step 1A<sup>7</sup>: correction to include all pyrrole moieties into the observed integration*

$$\text{final normalized integration} = \frac{\text{normalized integration from step 1}}{0.7}$$

*Step 2: calculation of the furfurylamine conversion*

$$\text{furfurylamine conversion} = \frac{\text{normalized integration product peak}}{\text{normalized integration product peak} + \text{normalized integration peak at 1.1 ppm}}$$

### A.2 Furfurylamine conversion using the results from Elemental Analysis

From Elemental Analysis, it was concluded that 1.72 w/w% of nitrogen atoms was present in the analysed PK-FU. This conclusion was used to calculate the furfurylamine conversion using the formulas shown below.

To start, a formula for the nitrogen conversion was defined:

$$\text{conversion } N = \frac{\text{mol } N \text{ in polymer}}{\text{mol } N \text{ in furfurylamine}} \quad [1]$$

In which:

$$\text{mol } N \text{ in polymer} = \frac{\frac{w}{w} \% N \text{ polymer} * \text{mass polymer}}{\text{molecular weight } N} \quad [2]$$

---

<sup>7</sup> This step was only performed for the signals corresponding to a R-group in the polymer backbone (1.1 and 1.9 ppm), see Figure 9 (II). Reason is that the signals only represent 70% of the pyrrole moieties present as the signal originates from the R-group being a methyl substituent. By dividing by 0.7, the case in which the R-group equals a hydrogen attached to either the polymer backbone or the pyrrole moiety is also taken into account.



And the mass of the polymer in [2] can be calculated using:

$$\text{mass polymer} = 30 + (\text{conversion } N * \text{mol furfurylamine} * \text{molecular weight furfurylamine}) - (2 * \text{conversion } N * \text{mol furfurylamine} * \text{molecular weight furfurylamine}) \quad [3]$$

Note that 30 g is the initial mass of the PK30 that underwent furan-grafting. The first term in brackets represents the weight that is added to the polymer due to integration of furfurylamine into the polymer backbone. The second term in brackets represent the weight that is lost by the polymer due to liberation of water molecules upon reaction.

Since the molecular weight of furfurylamine and the amount of moles furfurylamine added are known, see experimental procedure, [3] can be reduced to:

$$\text{mass polymer} = 30 + (2.782 * \text{conversion } N) \quad [4]$$

Substitution of [4] into [2] yields:

$$\text{mol } N \text{ in polymer} = 30 \left( \frac{\frac{w}{w} \% N \text{ polymer}}{\text{molecular weight } N} \right) + 2.782 \left( \frac{\frac{w}{w} \% N \text{ polymer} * \text{conversion } N}{\text{molecular weight } N} \right) \quad [5]$$

And finally, substitution of [5] into [1] yields a formula for the conversion of N:

$$\text{conversion } N \left( 1 - \frac{2.782 * \frac{w}{w} \% N \text{ polymer}}{\text{mol } N \text{ in furfurylamine} * \text{molecular weight } N} \right) = 30 \left( \frac{\frac{w}{w} \% N \text{ polymer}}{\text{molecular weight } N * \text{mol } N \text{ in furfurylamine}} \right)$$

$$\text{conversion } N = \frac{\frac{30 * \frac{w}{w} \% N \text{ polymer}}{\text{molecular weight } N * \text{mol } N \text{ in furfurylamine}}}{1 - \frac{2.782 * \frac{w}{w} \% N \text{ polymer}}{\text{mol } N \text{ in furfurylamine} * \text{molecular weight } N}} \quad [6]$$

Since all of the parameters in [6] are known, the conversion of N can be calculated to be: 87.5%. As 1 mol furfurylamine consists of 1 mol N, the conversion of N equals the conversion of furfurylamine. The conversion of the carbonyl moieties in the PK30 polymer can be calculated by using [7]. This amounts to a carbonyl conversion of 17.5%. Note that the maximum conversion of carbonyl moieties depends on the ratio of furfurylamine and carbonyl groups in PK30. It was given in the experimental that 1:5 ratio was used for respectively furfurylamine and the PK30 carbonyl-groups. Thus, the maximum conversion of carbonyl groups amounts to 0.2.

$$\text{conversion of carbonyl moieties} = \text{maximum conversion carbonyl moieties} * \text{conversion } N \quad [7]$$

### A.3 Hansen Solubility Parameter (HSP) estimation using group-contribution methods

Table 2 contains the Hansen Solubility Parameters (hereafter HSP) for different solvents, the PK-FU, anthracene, maleimide and the anthracene-maleimide adduct. Other than the HSP values obtained from literature, there is a column consisting of predicted HSP values. Calculations of these estimates was done using formulas and a general procedure from the work of Hansen [39]. Using the formula below, the different solubility parameters were estimated.

$$\delta = (\sum_i n_i F_i + \sum_j m_j S_j + 75954.1)^{0.383837} - 56.14 \quad [1]$$

In which:

$n_i$  = frequency of appearance for a certain first-order group

$F_i$  = the contribution of a first-order group

$m_j$  = frequency of appearance for a certain second-order group

$S_j$  = the contribution of a second-order group

The parameters  $F_i$  and  $S_j$  were obtained from literature [39]. In order to illustrate the calculations that were performed, an example is given below in which the HSP of PK-FU is estimated. Generally, the

full chemical structure of a compound can be used to estimate the corresponding HSP. However, for polymers, the assumption can be made that the repeating unit sufficiently represents the full structure regarding HSP estimation [54]. The different steps of the calculations are summarized below.

*Step 1: documentation of the contributing groups*

First-order groups	Contribution to $\delta$	Appearances in structural unit in Figure A-1 (II) if R=H	Appearances in structural unit in Figure A-1 (I) if R=H	Appearances in structural unit in Figure A-1 (II) if R=CH <sub>3</sub>	Appearances in structural unit in Figure A-1 (I) if R=CH <sub>3</sub>
CH <sub>3</sub>	-2308.6	0	0	2	1
CH <sub>2</sub>	-277.1	1	1	0	0
CH <sub>2</sub> CO	7274.2	1	1	1	1
CH<	-355.5	0	0	1	1
>C=C<	1601.8	0	0	1	0
>C=CH-	1887.1	3	0	2	0
CH=CH-	-381.9	1	0	1	0
C-O-C	-480.8	1	0	1	0

Table A-2| documentation of all first-order groups involved for the HSP estimation of PK-FU.

Second-order groups	Contribution to $\delta$	Appearances in structural unit in Figure A-1 (II)	Appearances in structural unit in Figure A-1 (I)
>N-CH <sub>2</sub>	-492.57	1	0

Table A-3| documentation of all second-order groups involved for the HSP estimation of PK-FU.

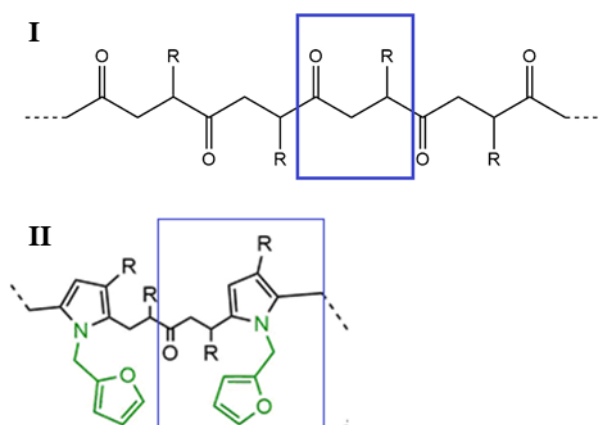


Figure A-1| the repeating units of the conventional (I) and furan-grafted (II) PK30.

For the first-order group contributions, the appearances were determined for four different cases:

- Case A: Conventional PK30 with R=H
- Case B: Conventional PK30 with R=CH<sub>3</sub>
- Case C: Furan-grafted PK30 with R=H
- Case D: Furan-grafted PK30 with R=CH<sub>3</sub>

In case of the second-order contributions, the distinction in R-groups only had to be made for PK-FU as the conventional PK30 did not contain the group shown in Table A-3. Using the group contributions

and the appearances per contribution, a total contribution for all four situations was calculated. Subsequently, the contributions were weighed in order to obtain the total contribution for a specific formulation of furan-grafted PK30. To illustrate, based on the percentage of furan-grafting (obtained from <sup>1</sup>H-NMR and Elemental Analysis) the polymer backbone was divided in two regions. The furan-grafting of 15.4% implied that 15.4% of the total contribution would be accounted for by cases C and D. And subsequently, 30% of the contribution of cases C and D was accounted for by case C and 70% by case D as PK30 generally consists of 30% ethylene. The same procedure was followed for the remaining 84.6% of conventional PK30. Finally, the weighed first-order- and second-order contributions were substituted into [1] and the HSP was calculated.

The same procedure was followed for solvents, maleimide and the maleimide-anthracene adduct. For these cases, the chemical structure was used to determine group-contribution appearances and no weighing was needed in order to calculate the HSP.

#### A.4 Concentration determination using the Lambert-Beer law

After determination of the molar decadic extinction coefficient ( $\epsilon$ ), the Lambert-Beer law (shown below) was used to determine the UV-vis samples' polymer concentration.

$$A = \epsilon * c * l$$

$$c = \frac{A}{\epsilon * l} \quad [1]$$

In which:

$c$  = the concentration in the examined UV-vis sample (mg/mL)

$A$  = the absorbance in the UV-vis spectrum (factor, not percentage)

$\epsilon$  = the molar decadic extinction coefficient (cm<sup>2</sup>/mg)

$l$  = the pathlength of light travel in the cuvette (cm), typically 1 cm

For a particular solvent, [1] can be used to calculate the concentration of PK-FU in the examined UV-vis sample. As was stated before, the absorbance at 500 nm solely represents the amount of PK-FU present in the solvent. An example calculation is shown below.

##### *Calculation of the polymer concentration in a UV-vis sample*

Using the procedure described in the experimental,  $\epsilon$  was determined for PK-FU dissolution in toluene:

$$\epsilon = 4.78 * 10^3 \text{ cm}^2/\text{mg}$$

Also, UV-vis analysis of the yielded the absorbance for the polymer-solvent-anthracene sample:

$$A = 0.8$$

Then, knowing that the typical pathlength of light in the cuvette equals 1 cm, the concentration can be calculated using [1]:

$$c = \frac{A}{\epsilon * l} = \frac{0.8}{(4.78 * 10^3) * 1} = 0.1674 * 10^{-3} \frac{\text{mg}}{\text{mL}} = 0.1674 \frac{\text{mg}}{\text{L}}$$

In case the sample's polymer concentration is too high, the Lambert-Beer law becomes inapplicable due to the occurrence of non-proportionality between the concentration and the absorption. In order to still be able to apply the Lambert-Beer law, the sample has to be diluted. An example of such a situation is described below.

*Calculation of high polymer concentrations in a UV-vis sample*

The extinction coefficient for the toluene-polymer mixture remains the same:

$$\varepsilon = 4.78 \cdot 10^3 \text{ cm}^2/\text{mg}$$

A highly concentrated sample yields a relatively high absorbance in the UV-vis spectrum:

$$A = 3.0$$

Due to non-proportionality of the absorbance and the sample concentration at this absorbance value, the Lambert-Beer law cannot be applied directly. Therefore, it is chosen to dilute the sample ten times by addition of nine sample-volumes solvent. This yields a sample with a new absorbance:

$$A = 0.6$$

Using this absorbance, the concentration of the diluted sample can be calculated using [1]:

$$c = \frac{A}{\varepsilon \cdot l} = \frac{0.6}{4.78 \cdot 10^3 \cdot 1} = 0.1255 \cdot 10^{-3} \frac{\text{mg}}{\text{mL}} = 0.1255 \frac{\text{mg}}{\text{L}}$$

And since the sample was diluted ten times, so the concentration of the original sample will be ten times the calculated concentration:

$$c_{\text{original}} = c_{\text{diluted}} \cdot \text{dilution factor} = 0.1255 \cdot 10 = 1.255 \frac{\text{mg}}{\text{L}}$$